

DOI: 10.1515/amm-2017-0040

G. GOLAŃSKI[#], J. JASAK^{*}, A. ZIELIŃSKI^{**}, C. KOLAN^{*}, M. URZYNICOK^{***}, P. WIECZOREK^{*}**QUANTITATIVE ANALYSIS OF STABILITY OF 9%Cr STEEL MICROSTRUCTURE AFTER LONG-TERM AGEING**

The paper presents the results of research on the microstructure of martensitic X10CrMoVNb9-1 (P91) and X13CrMoCoVNbNB9-2-1 (PB2) steel subject to long-term ageing at the temperature of 620°C and holding times up to 30 000 hours. The microstructural tests of the examined steel types were performed using a scanning microscope Joel JSM – 6610LV and a transmission electron microscope TITAN 80 – 300. The stability of the microstructure of the investigated steels was analyzed using a quantitative analysis of an image, including measurements of the following: the density of dislocations inside martensite/subgrain laths, the width of martensite laths, and the mean diameter of precipitates. It has been concluded that during long-term ageing, the microaddition of boron in PB2 steel significantly influenced the slowing of the process of degradation of the martensitic steel microstructure, as a result of slowing the process of coagulation of $M_{23}C_6$ carbides and Laves phase. It had a favorable effect on the stabilization of lath microstructure as a result of retardation of the processes of recovery and polygonization of the matrix.

Keywords: High-chromium martensitic steels, microstructure, carbide precipitation.

1. Introduction

High-chromium martensitic steels of the 9-12%Cr type are currently one of the basic construction materials used when building new power units for the super- and ultra supercritical parameters and when modernizing/repairing the conventional power units. Previous experience from the use of martensitic 9%Cr steels in the power industry – P/T91, P92 and E911 steels, shows that the main mechanism of degradation of these steels are the processes of coagulation of $M_{23}C_6$ carbides and the precipitation and growth of Laves phase on the boundaries [1-3]. The $M_{23}C_6$ carbides in the microstructure of 9%Cr steel fulfill a very significant role as a factor stabilizing the martensitic lath microstructure. However, because of their low thermodynamic stability, they are characterized by the susceptibility to coagulation, which causes a disappearance of both the effect of anchoring of subgrain boundaries by these precipitates and the progressing process of polygonization of the matrix. The precipitation and fast growth of Laves phase particles on the boundaries leads to a decrease in the crack resistance and an increase in the steel brittleness. On the other hand, matrix depletion of the substitution elements (chromium, molybdenum, tungsten), as a result of their diffusion to the precipitating Laves phase, increases the steel susceptibility to the process of recovery and polygonization of the matrix, and reduces the resistance to oxidation [2-5]. A partial antidote to the mentioned negative effect of $M_{23}C_6$ and Laves phase precipitates is introducing the microaddition of boron into

the martensitic steels. Boron partly replaces carbon atoms in the $M_{23}C_6$ carbide, forming more stable carbon borides $M_{23}(C, B)_6$, which coagulate slower during the service and additionally have an influence on the increase in dispersion of these precipitates. Boron was observed to have a similar positive effect on slowing down the precipitation and increasing the stability of Laves phase [2,5-7]. The result of such an approach to designing was the modification of the chemical composition of 9%Cr steel consisting in the introduction of the boron microaddition to the chemical composition, the result of which was developing a group of materials including X13CrMoCoVNbNB9-2-1 (PB2) steel [8].

The aim of the work was to compare the results of influence of long-term ageing on the changes in the microstructure of 9%Cr steel – the X10CrMoVNb9-1 (P91) steel of the first generation and the X13CrMoCoVNbNB9-2-1 (PB2) steel being the next modification of this steel group. The paper presents the results of research on the microstructure and its quantitative analysis with the use of transmission electron microscopy.

2. Material and methodology of research

The material for testing was samples taken from the pipe sections of X10CrMoVNb9-1 (P91) steel and X13CrMoCoVNbNB9-2-1 (PB2) steel, of the respective measurements: 160×16.8 mm and 219×32 mm. The chemical composition of the investigated steels, determined by means of a spark spectrometer

^{*} CZESTOCHOWA UNIVERSITY OF TECHNOLOGY, INSTITUTE OF MATERIALS ENGINEERING, 19 ARMII KRAJOWEJ AV., 42-200 CZĘSTOCHOWA, POLAND

^{**} INSTITUTE OF FERROUS METALLURGY, 12-14 K.MIARKI STR., 44-100 GLIWICE, POLAND

^{***} BOILER ELEMENTS FACTORY "ZELKOT", KOSZĘCIN, POLAND

[#] Corresponding author: grisza@wip.pcz.pl

Chemical composition of the examined steels, wt%

Steel	C	Si	Mn	Cr	Mo	V	Nb	N	Co	P	S	B
P91	0.11	0.42	0.51	9.12	0.93	0.22	0.077	0.05	—	0.018	0.0040	—
PB2	0.14	0.11	0.34	9.42	1.55	0.19	0.057	0.04	1.38	0.011	0.0008	0.008

Spectro K2 Analytical Instruments, is presented in Table 1. The examined steels were subject to ageing at the temperature of 620°C and holding time up to 30 000 hours. The ageing temperature of 620°C, according to authors [8], is the maximum acceptable temperature of service for PB2 steel.

The microstructural tests were carried out using a scanning microscope (SEM) Joel JSM – 6610LV and a transmission electron microscope (TEM) TITAN 80 – 300 with the accelerating voltage of 220 kV. Observation of the microstructure was made for the chosen times of ageing at the temperature of 620°C, i.e. the as-received state and after 30 000 hours of ageing. The observation and record of images of the P91 and PB2 steel microstructures by means of the scanning microscope was performed on metallographic specimens etched with ferrous chloride as an etchant.

The tests with the transmission electron microscope were carried out using thin foils. The identification of the precipitates was realized with the use of selected electron diffraction. The measurements of the density of free dislocations inside the subgrains and the mean width of martensite laths were taken on the microstructure images. The quantitative analysis was made with the computer image analysis using the Analysis software.

3. The results of research and discussion

Microstructure of the steel in the as-received state

In the as-received condition, the examined steels were characterized by the microstructure of high-tempered martensite with numerous carbides. The precipitates were seen mostly on

the boundaries of prior austenite grains, on the lath boundaries, and inside martensite laths (Fig. 1). The relative number of carbides was bigger than in the PB2 steel, which probably results from the higher content of carbon in this steel (Table 1) and the applied parameters of heat treatment. In the microstructure of the examined steels, delta ferrite was not observed. The microstructure of these materials was a typical microstructure for this steel grade [1,4-5].

The observations of the microstructure of the investigated steels in the as-received state made under magnification of the transmission electron microscopy revealed the occurrence of lath microstructure of tempered martensite having the subgrain structure with high density of free dislocations inside the subgrains and with numerous precipitates (Fig. 2). The estimated mean density of free dislocations in P91 and PB2 steels in the as-received condition was similar and amounted to $1.21 \times 10^{14} \text{ m}^{-2}$ and $1.23 \times 10^{14} \text{ m}^{-2}$, respectively. Moreover, in the microstructure of these steels, the occurrence of the areas of polygonized ferrite was revealed. The observations by TEM also proved that some of the subgrain boundaries were not filled with carbides (Fig. 2). Literature data [9-10] show that the subgrain boundaries of the misorientation angle below 20° are not the areas of preferential precipitation of carbides. According to research [10], only about 8% of M_{23}C_6 carbides were precipitated on the small-angle boundaries of the misorientation angle amounting to 8÷15°. The boundaries of small angle constitute at least 60% of the overall number of boundaries in the tempered martensite. Small misorientation angle of the boundaries contributes to their low mobility, which ensures relative stability of the subgrain substructure [9]. The mobility of the boundaries of small angle (2÷5°) is at least three orders of magnitude as low compared with the boundaries of large angle

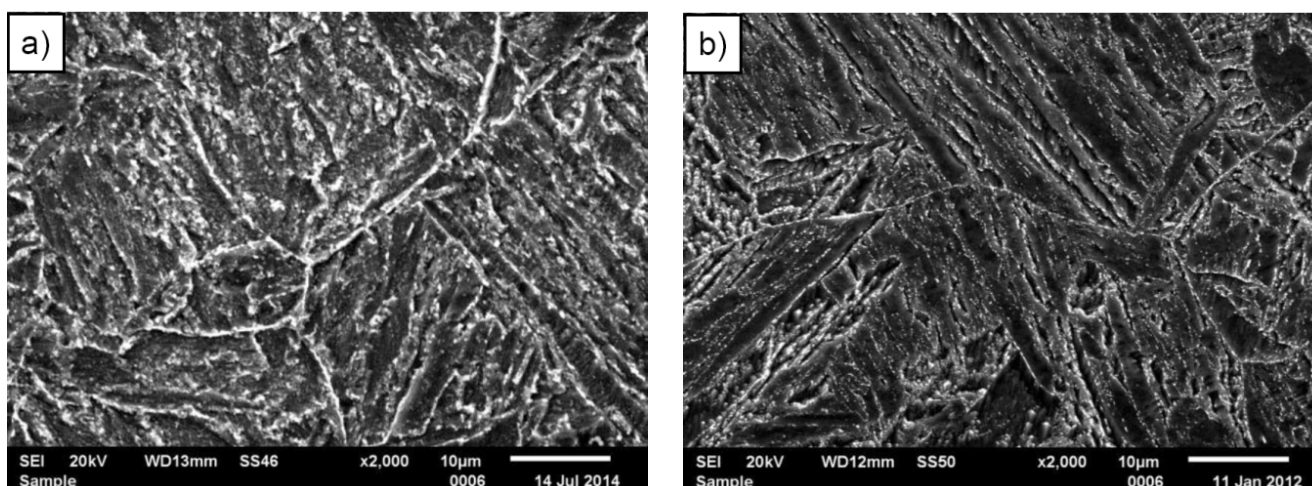


Fig. 1. Microstructure of the examined steels in the as-received state: a) P91; b) PB2, SEM

[9,11]. It probably results from the lower energy on the boundary of small angle in comparison with the boundaries of large angle. The mean width of martensite laths in P91 steel in the as-received state amounted to 487 nm, whereas in PB2 steel – 432 nm.

In the examined steels in the as-received condition, the following precipitate types were observed: $M_{23}C_6$ carbides, as well as carbides and carbonitrides of the MX type. The examples of the precipitates revealed in the investigated steels are shown in (Figs. 3-6).

It has been proved that in the examined steels, the $M_{23}C_6$ carbides (Figs. 3, 4) were most of all precipitated on the boundaries of prior austenite grain and on the boundaries of subgrains/martensite laths. Only few of them were seen inside ferrite subgrains. The mean width of $M_{23}C_6$ precipitates in P91 steel in the as-received state amounted to 106 nm, whereas for PB2 steel, it was lower and amounted to 76 nm. The $M_{23}C_6$ carbides precipitated on the boundaries of subgrains/martensite laths fulfill a significant role in the processes of ageing. They inhibit the movement of dislocation boundaries and at the same time stabilize the subgrain microstructure of martensite [4,11]. The

$M_{23}C_6$ carbides in high-chromium steels of the 9÷12%Cr type after heat treatment are the dominant precipitation and constitute around 90% of all precipitates [12].

In the case of precipitates of the MX type, two morphologies were distinguished: the spherical ones rich in niobium – NbC carbides, and the lamellar ones, rich in vanadium – VX precipitates (nitrides/carbonitrides) (Figs. 5, 6). In the investigated steels, there was no occurrence of complex precipitates called „V-wings”, consisting of a spherical NbC precipitate and lamellar VX nitrides nucleating on it. Literature data [2,6,9,13] indicate that the precipitate of this type can occur in steels of 9%Cr content. The fine-dispersion precipitates of the MX type were in turn observed inside the subgrains. The MX particles revealed inside the subgrains were mostly precipitated on the dislocations. The mean width of the MX-type precipitates in P91 steel in the as-received condition amounted to 32.4 nm, whereas in PB2 steel – 25.7 nm. Fine-dispersion precipitates of the MX type (NbC, VX), which were precipitated inside martensite laths, anchor and impede the movement of dislocations, ensuring high creep resistance [13]. The spheroidal particles of NbC carbides

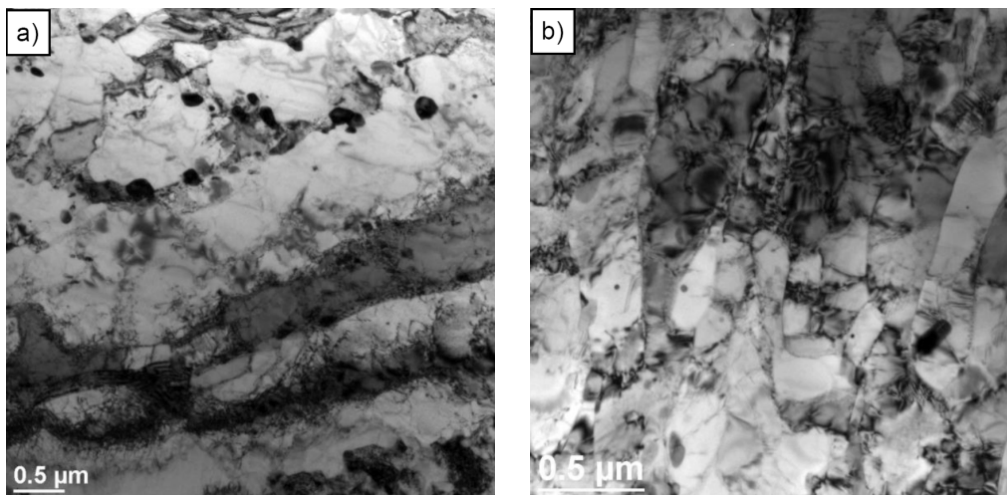


Fig. 2. The microstructure of the examined steels in the as-received state: a) P91; b) PB2, TEM

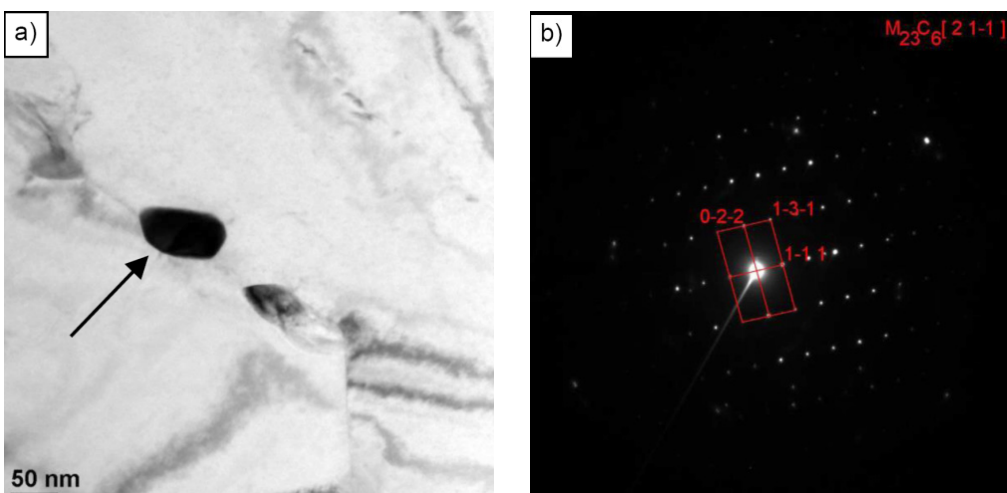


Fig. 3. $M_{23}C_6$ carbide in the microstructure of P91 steel in the as-received state: a) bright field; b) solved electron diffractogram of $M_{23}C_6$ carbide with the zone axis

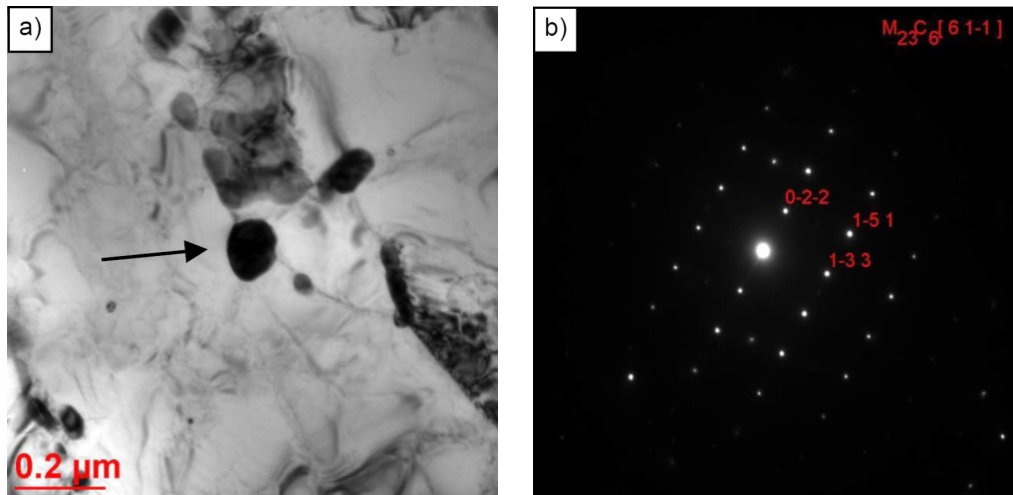


Fig. 4. $M_{23}C_6$ carbide in the microstructure of PB2 steel in the as-received state: a) bright field; b) solved electron diffractogram of $M_{23}C_6$ carbide with the zone axis

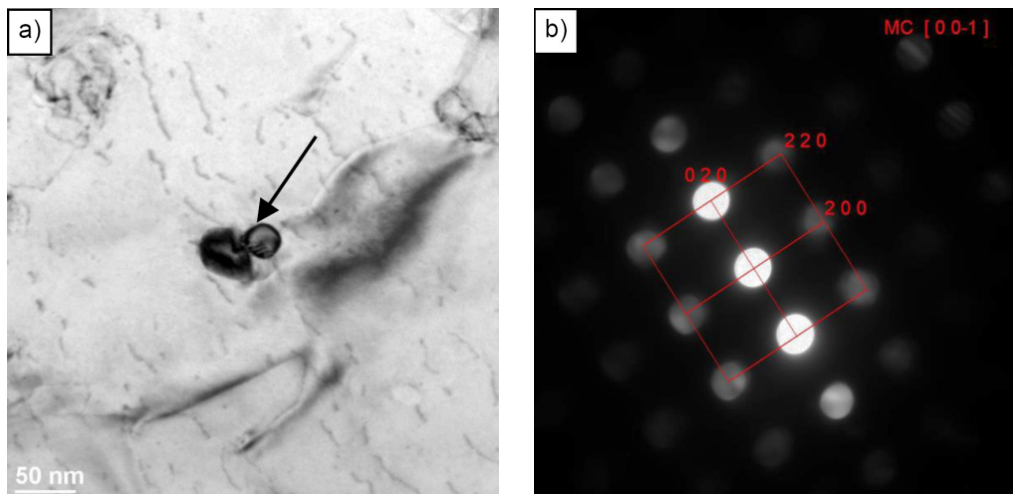


Fig. 5. MC carbide in the microstructure of P91 steel in the as-received state: a) bright field; b) solved electron diffractogram of MC carbide with the zone axis

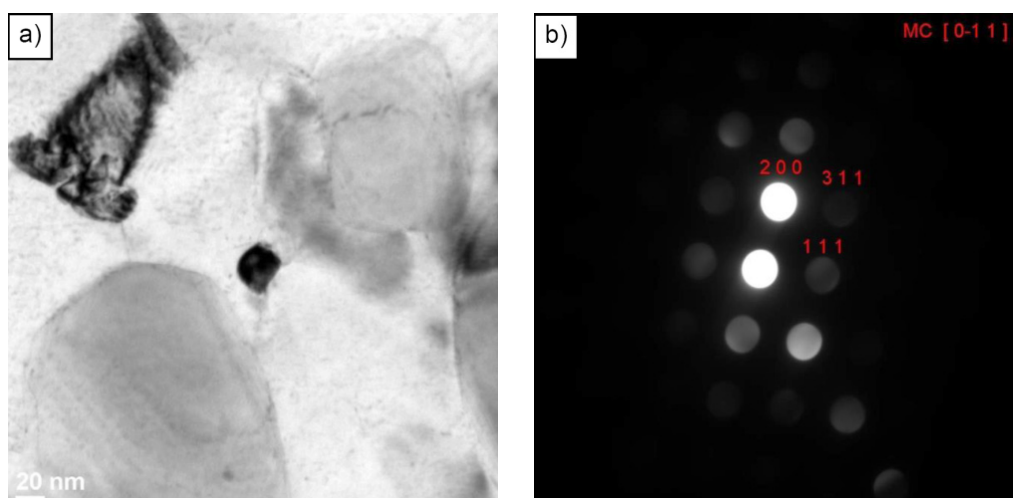


Fig. 6. MC carbide in the microstructure of PB2 steel in the as-received state: a) bright field; b) solved electron diffractogram of MC carbide with the zone axis

do not dissolve during austenitizing, thereby inhibiting the grain growth and increasing the ductility and strength of the 9-12%Cr steel [13, 14].

Microstructure of P91 and PB2 steels after long-term ageing

Martensitic steels of the 9%Cr type in the hardened and tempered state have a metastable microstructure that is going to evolve influenced by the temperature and time – ageing and by the stresses – creeping.

Long-term ageing of P91 and PB2 steel for the time of up to 30 000 hours, compared with the as-received state, most of all resulted in a visible relative growth of the number and size of particles precipitated on the boundaries of prior austenite grain, on the boundaries of subgrains, and inside subgrains (Fig. 7). The number of precipitates on the boundaries of prior austenite grain was so large that they formed the so-called continuous grid in some places. The precipitation processes were more advanced in the case of the aged P91 steel.

Observations by TEM showed a partly retained lath arrangement of martensitic microstructure after long-term ageing. However, the areas of polygonized ferrite were also noticed (Fig. 8). Ageing of the investigated steels contributed to the changes in their dislocation microstructure. The mean density of free dislocations in P91 steel after 30 000 hrs of ageing at the temperature of 620°C amounted to $0.78 \times 10^{14} \text{ m}^{-2}$, whereas in PB2 steel – $1.05 \times 10^{14} \text{ m}^{-2}$. The estimated fall of the dislocation density was connected with the processes of recovery and polygonization of the matrix and it was a result of their regrouping to the low-energy configurations and annihilation in the boundaries. These changes can occur as a result of climbing of the edge dislocations and cross slip of the screw dislocations.

In the examined steels after ageing, also the interaction of the dislocations inside the subgrains with fine-dispersion MX precipitates and $M_{23}C_6$ carbides was observed (Fig. 9).

The changes in the dislocation microstructure lead to an increase in the size of subgrains that occurs as a result of the migration or coalescence of the subgrains. The growth of the size of subboundaries usually takes place by the „Y”-type mechanism [15]. Migration by this mechanism consists in the movement of

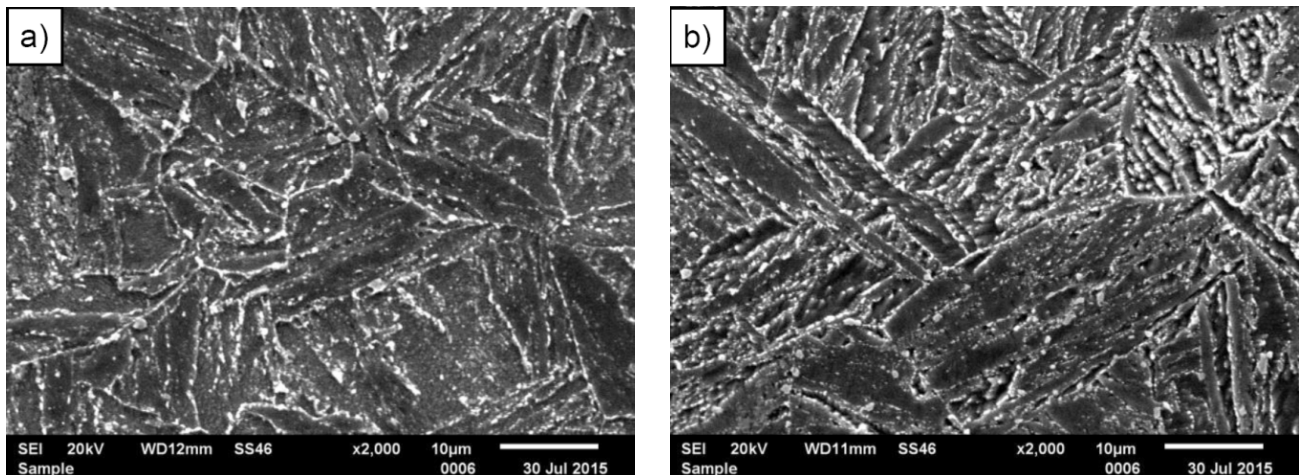


Fig. 7. Microstructure of the examined steels after ageing: a) P91; b) PB2, SEM

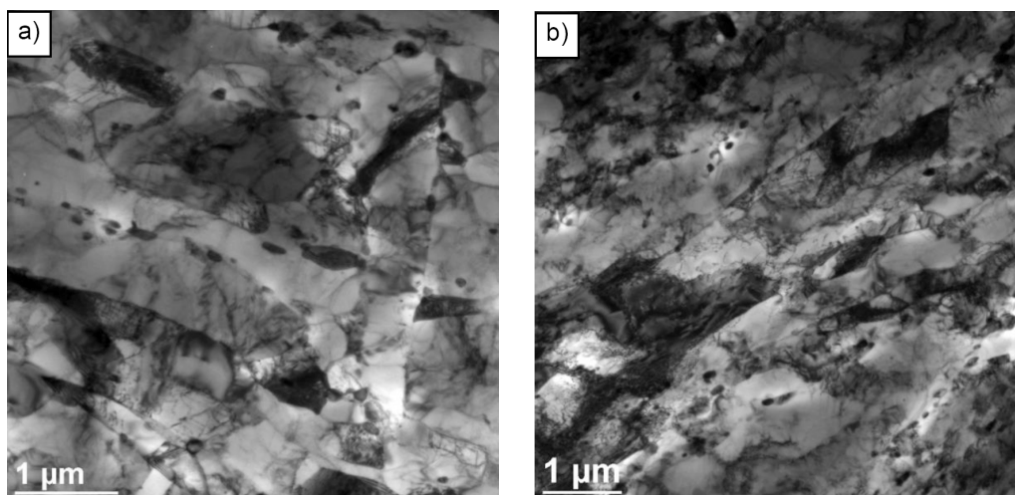


Fig. 8. Microstructure of the examined steels after ageing: a) P91; b) PB2, TEM

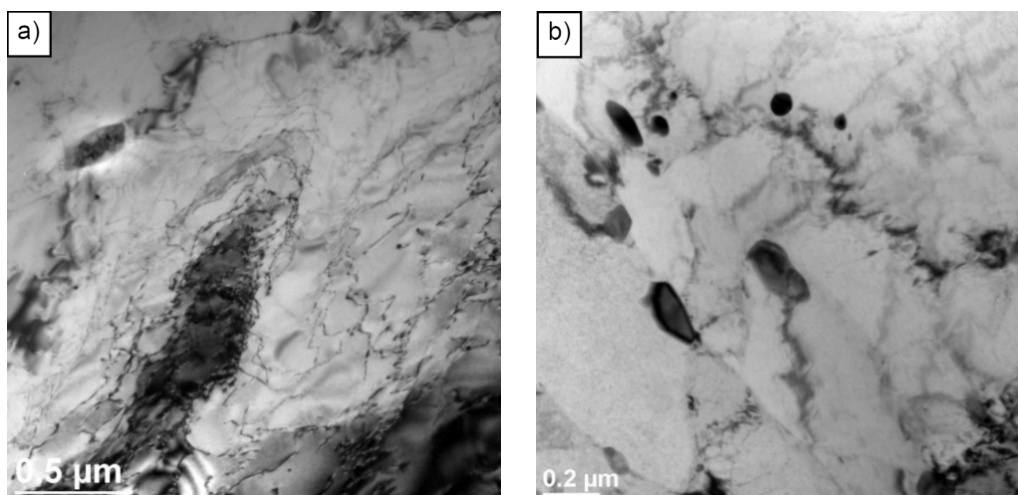


Fig. 9. Interaction of dislocations with: a) fine-dispersion MX precipitates inside the subgrains in PB2 steel, b) $M_{23}C_6$ carbides in P91 steel, TEM

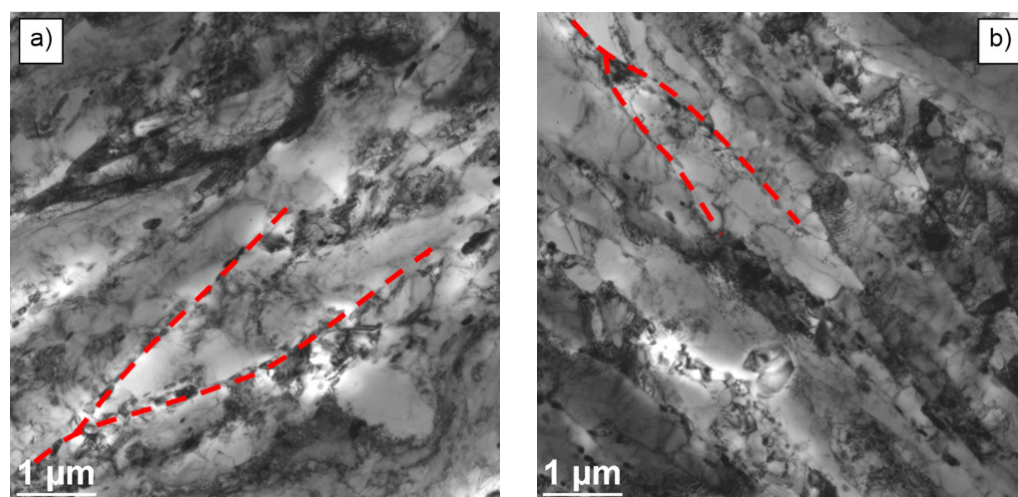


Fig. 10. Morphology of „Y” nodes in: a) P91 steel, b) PB2 steel, TEM

„Y” nodes being the points of contact of three subboundaries, which enables the coalescence of two small-angle boundaries (Fig. 10).

In the microstructure, the areas with the presence of both wide and narrow laths of martensite were observed. The narrow laths were seen in the microareas of large number of $M_{23}C_6$ precipitates on the boundaries (Fig. 11). It confirms the important role of these precipitates as a factor stabilizing the lath microstructure of tempered martensite. The precipitate – free boundaries show greater mobility, which leads to the growth of their width [9,11]. The mean width of martensite laths in the aged steels was bigger compared with that in the as-received state and amounted to 599 and 539 nm, respectively, for P91 and PB2 steel.

The microstructural tests with the use of TEM showed the occurrence of numerous precipitates on the boundaries of prior austenite grain and on the boundaries of laths, and they formed the so-called continuous grid of precipitates in some places (Fig. 12). Long-term ageing of the examined steels also contributed to a change in the morphology and type of precipitates. Similarly as in the as-received state, in their microstructure, not

only $M_{23}C_6$ carbides were seen, but also the MX-type precipitates. The dominant type of precipitates, just as in the as-received condition, were the chromium-rich $M_{23}C_6$ carbides. These precipitates were noticed on the boundaries of prior austenite grain, on the boundaries of subgrains, as well as inside the subgrains. The inside of the subgrains was also where the MX-type precipitates were seen. The mean diameter of $M_{23}C_6$ carbides after 30 000 hours of ageing amounted to around 160 nm – in P91 steel and 96 nm – in PB2 steel, whereas for the MX precipitates: 34 nm in P91 steel and 26 nm in PB2 steel. The increase in the size of $M_{23}C_6$ carbides, with the assumption of their constant volume fraction, according to Ostwald’s law, leads to a reduction of their number and contributes to their non-homogeneous distribution (Fig. 8). In consequence, the $M_{23}C_6$ carbides become a less effective factor stabilizing and controlling the growth of the subgrain size. A slight growth of the size of $M_{23}C_6$ carbides in PB2 steel, compared with P91 steel, indicates a positive influence of the boron microaddition on the stability of these precipitates. Boron segregates to the boundaries of prior austenite grain and other defects of the microstructure, decreasing their energy. Thus

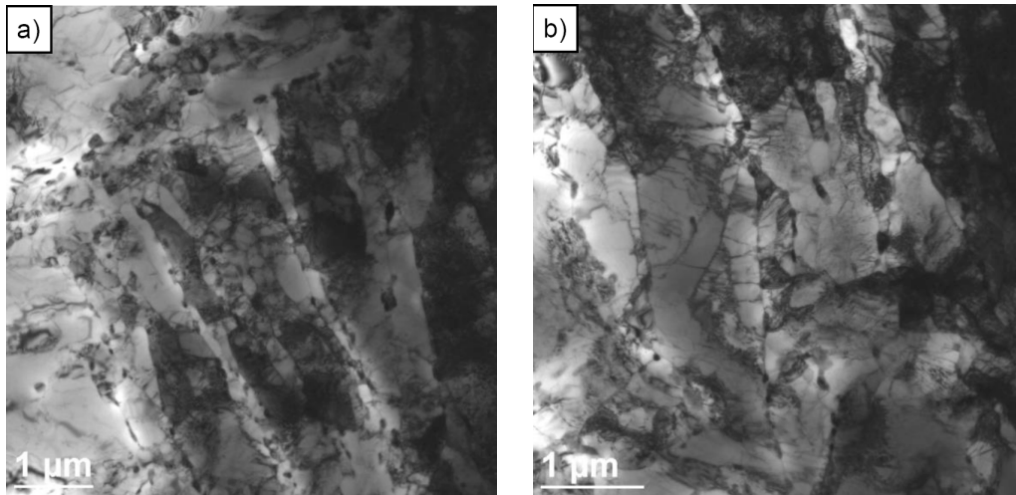


Fig. 11. Microstructure of the examined steels with visible wide and narrow laths of martensite: a) P91 steel, b) PB2 steel, TEM

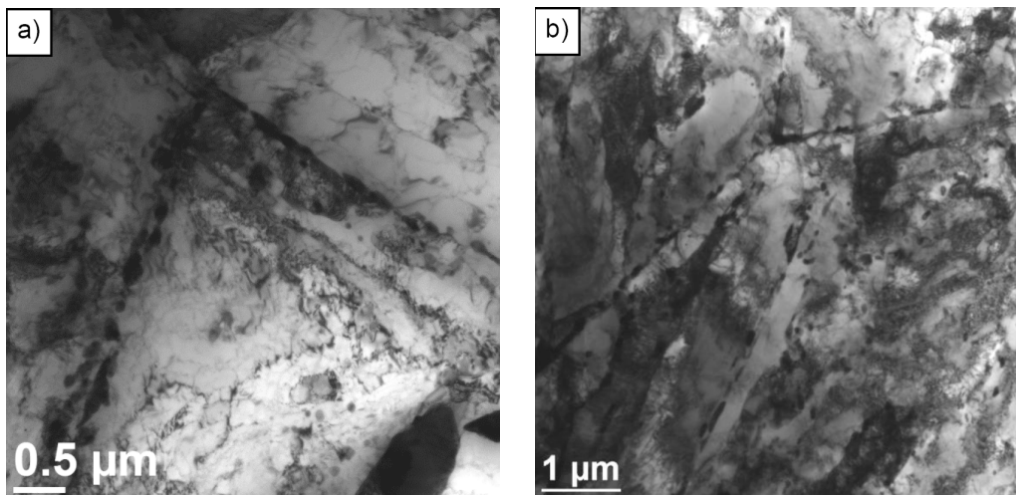


Fig. 12. Continuous grid of precipitates on the boundaries of prior austenite grain: a) P91 steel, b) PB2 steel, TEM

the atoms of boron can also segregate to the interphase boundary $M_{23}C_6$ carbide/matrix contributing to a decrease in energy, which results in a reduction of the precipitates coagulation rate [16]. Therefore, it can be assumed that boron uncombined in the precipitates but dissolved in the matrix can significantly influence the stability of the microstructure. According to [7,9], apart from boron combined in the precipitates, a few ppm of dissolved element remain in ferrite.

The comparable mean diameter of the precipitates of the MX type in the examined steels proves their high stability during long-term annealing. Apart from the precipitates mentioned above, i.e. $M_{23}C_6$ and MX, there were two types of secondary precipitates revealed additionally in the investigated steels: the precipitates of Laves phase (Fig. 13) and compound chromium nitride $Cr(V, Nb)N-Z$ phase (Fig. 14). The Laves phase precipitates in the investigated steels after ageing were mostly observed on the boundaries of prior austenite grain, usually near $M_{23}C_6$ carbides, and on the boundaries of subgrains (Fig. 13).

The precipitation and growth of Laves phase is a very unfavorable phenomenon and is regarded as the main mechanism of

degradation of 9%Cr-type steel [17]. The precipitates of Laves phase were observed in the steels of the 9%Cr type already after around 500 hours of creep [18,19]. Laves phase is characterized by a high proneness to coagulation [19]. The precipitation and fast growth of this phase due to its low stability contributes to the matrix depletion of chromium and molybdenum atoms. It leads to the fall of solution strengthening of the matrix and at the same time increases the steel susceptibility to the processes of recovery and polygonization of the matrix. However, the matrix depletion of substitution elements, being also the components of $M_{23}C_6$ carbides, has a favorable influence on slowing down of the coagulation process of these precipitates [17,20].

Precipitated on the boundaries of grains, the particles of $M_{23}C_6$ and Laves phase also contribute to a decrease in ductility and growth of the nil ductility transition temperature [21]. Performed measurements show that the mean diameter of the Laves phase precipitates in P91 steel amounted to around 1234 nm (1.234 μm), whereas in PB2 steel it was nearly twice as low and amounted to 680 nm (0.680 μm). Smaller size of the Laves phase precipitates in PB2 steel after ageing proves a positive

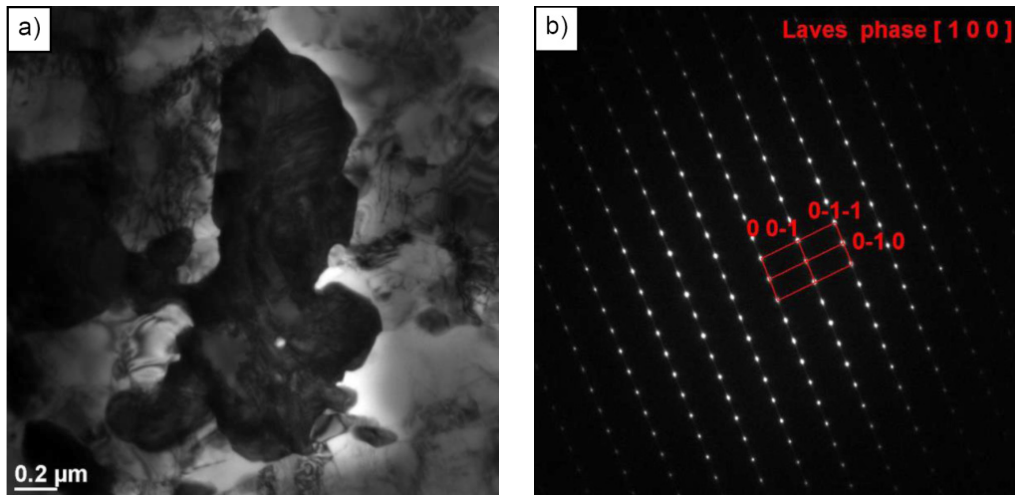


Fig. 13. Laves phase precipitate in the microstructure of w P91 steel after 30 000 hours of ageing: a) bright field; b) solved electron diffractogram of the Laves phase precipitate with the zone axis

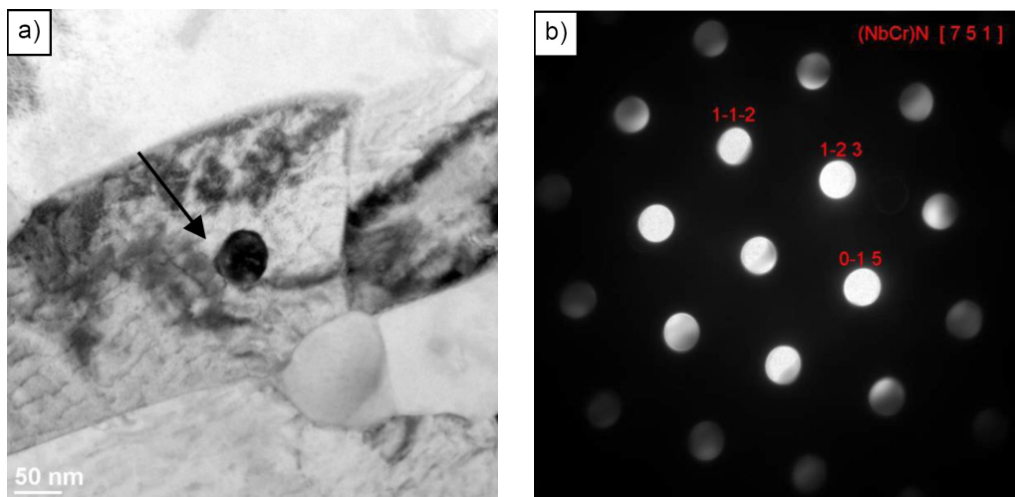


Fig. 14. Z phase precipitate in the microstructure of P91 steel after 30 000 hours of ageing: a) bright field; b) solved electron diffractogram of the Z phase precipitate with the zone axis

influence of the boron microaddition on the stability increase in these precipitates.

In P91 steel, also single precipitates of Z phase, that is a compound nitride $\text{Cr}(\text{V}, \text{Nb})\text{N}$, were noted (Fig. 14). Precipitates of this type, however, were not observed in PB2 steel. The precipitation of Z phase occurs as a result of dissolving fine-dispersion precipitates of the MX type in the matrix, causing a fall of the precipitation strengthening with these particles.

It is assumed that every large precipitate of Z phase is formed as a result of the disappearance of around 1500 fine-dispersion MX particles [22,23]. It leads to a decrease in the density of occurrence of these precipitates and to the growth of the distance between them, which has a negative influence on creep strength. The susceptibility to precipitation of this unfavorable phase grows together with the increase in the chromium and niobium content in the steel [22,24]. In the steels of 9%Cr type, Z phase is a coherent precipitation. Its size is similar to the MX-type precipitates and it usually occurs in the microstructure

in the form of single particles [22,24]. Therefore, its influence on the properties of these steels is minor. In the examined steel, however, the inhibiting effect of MX-type precipitates on the movement of dislocations was still noted (Fig. 11). The mean diameter of the Z phase precipitates in P91 steel after ageing amounted to around 58 nm.

3. Conclusions

1. In the as-received state, P91 and PB2 steels were characterized by the microstructure of tempered martensite with numerous precipitates and high dislocation density. On the boundaries of prior austenite grain and tempered martensite laths, the M_{23}C_6 carbides were precipitated. Inside martensite laths, however, the precipitates of the MX type – VX and NbC, as well as single M_{23}C_6 carbides were observed.

2. Long-term ageing of P91 and PB2 steels at the temperature of 620°C contributed to the following changes in the microstructure:
 - the growth of the width of tempered martensite laths and the fall of the dislocation density;
 - the preferential precipitation of $M_{23}C_6$ carbides on the boundaries of prior austenite grain and on the boundaries of martensite laths, and their coagulation;
 - the precipitation and growth of Laves phase and in the case of P91 steel also the precipitation of Z phase.
 3. The fine-dispersion precipitates of the MX type were stable during long-term ageing.
 4. The microaddition of boron in PB2 steel had a significant influence on the slowdown of the process of degradation of its microstructure through:
 - stabilization of the $M_{23}C_6$ carbides and Laves phase precipitates, contributing to the slowdown of the process of their coagulation;
 - retardation of the processes of recovery and polygonization of the matrix.
- REFERENCES
- [1] A. Zieliński, M. Miczka, B. Boryczko, M. Sroka, *Arch. Civ. Mech. Eng.* **4**, 813-824 (2016).
 - [2] C.G. Panait, W. Bendick, A. Fuchsmann, A.F. Gourgues-Lorenzon, J. Besson, *Inter. J. Pres. Ves. Piping* **87**, 326-335 (2010).
 - [3] P. Duda, Ł. Felkowski, J. Dobrzański, H. Purzyńska, *Materials at High Temperatures* **33**, 85-93 (2016).
 - [4] W. Yan, W. Wang, Y.Y. Shan, K. Yang, *Front. Mater. Sci.* **7**, 1-27 (2013).
 - [5] M. Yoshizawa, M. Igarashi, K. Moriguchi, A. Iseda, H.G. Armaki, K. Maruyama, *Mater. Sc. Eng. A* **510-511**, 162-168 (2009).
 - [6] F. Abe, T. Horiuchi, M. Taneike, K. Sawada, *Mater. Sc. Eng. A* **378**, 299-303 (2004).
 - [7] K. Bryła, K. Spiradek-Hahn, A. Zielińska-Lipiec, H. Firganeck, P.J. Ennis, A. Czyrska-Filemonowicz, *Inżynieria Materiałowa* **3**, 702-705 (2004).
 - [8] A.Di Gianfrancesco, L. Cipolla, D. Venditti, S. Neri, M. Calderini, *ECCC CreepConference, Zurich*, 919-934 (2009).
 - [9] A. Zielińska-Lipiec, *Stale stosowane w energetyce konwencjonalnej i jądrowej, Wybrane zagadnienia*, 2015 AGH, Cracow.
 - [10] Y. Xu, X. Zhang, Y. Tian, C. Chen, Y. Nan, H. He, M. Wang, *Mater. Character.* **111**, 122-127 (2016).
 - [11] H. Ghassemi-Armaki, R.P. Chen, K. Maruyama, M. Yoshizawa, M. Igarashi, *Mater. Let.* **63**, 2423-2425 (2009).
 - [12] J.G. Zhang, F.W. Noble, B.L. Eyre, *Mater. Sc. Techn.* **7**, 218-223 (1991).
 - [13] F. Abe, *Science and Technology of Advanced Materials* **9**, 1-15 (2008).
 - [14] G. Golański, A. Zieliński, A. Zielińska-Lipiec, *Materialwiss. Werkst.* **46**, 248-255 (2015).
 - [15] F. Abe, *Mater. Sc. Eng. A* **387-389**, 565-569 (2004).
 - [16] M. Hättstrand, H.O. Andrén, *Mater. Sc. Eng. A* **270**, 33-37 (1999).
 - [17] J.S. Lee, H.G. Armaki, K. Maruyama, T. Muraki, H. Asahi, *Mater. Sc. Eng. A* **428**, 270-275 (2006).
 - [18] X. Guo, J. Gong, Y. Jiang, D. Rong, *Mater. Sc. Eng. A* **564**, 199-205 (2013).
 - [19] M. Hättstrand, H.O. Andrén, *Micron* **32**, 789-797 (2001).
 - [20] G. Golański, A. Zielińska-Lipiec, S. Mroziński, C. Kolan, *Mater. Sc. Eng. A*, **627**, 106-110 (2015).
 - [21] A. Zieliński, G. Golański, M. Sroka, *Kovove Mater.* **54**, 61-70 (2016).
 - [22] H.K. Danielsen, J. Hald, *VGB Power Tech.* **5**, 68-73 (2009).
 - [23] H.K. Danielsen, J. Hald, *Energy Materials* **1**, 49-57 (2006).
 - [24] R.O. Kaibyshev, V.N. Skorobogatykh, I.A. Shchenkova, *Metal Science and Heat Treatment* **52**, 90-99 (2010).